FACTA UNIVERSITATIS
Series: **Mechanical Engineering** Vol. 22, Nº 2, 2024, pp. 329 - 342
https://doi.org/10.22190/FUME240605035H

Original scientific paper

A FRACTAL-BASED APPROACH TO THE MECHANICAL PROPERTIES OF RECYCLED AGGREGATE CONCRETES

Chun-Hui He[1], Hua-Wei Liu[1], Chao Liu[1,2]

[1]School of Civil Engineering, Xi'an University of Architecture and Technology, Xi'an, China
[2]School of Science, Xi'an University of Architecture and Technology, Xi'an, China

ORCID iDs: Chun-Hui He https://orcid.org/0000-0003-0810-5248
Hua-Wei Liu https://orcid.org/0000-0003-4433-5075
Chao Liu https://orcid.org/0000-0002-9634-7791

Abstract. *The mechanical properties of porous concrete, such as strength and durability, are significantly influenced by moisture transport, particularly in the case of recycled aggregate concretes. The pore distribution and pore size of the concrete, as well as the ambient temperature in the surrounding environment, exert a significant influence on the moisture transport. This paper establishes the fractal Fick's law, the fractal Darcy law, and the fractal Richards equation. In conclusion, a fractal model for the diffusion and permeability in porous concrete is established. This study examines the mechanisms of moisture diffusion and water permeability in concrete. The comparison of the theoretical prediction with the experimental data indicates a high degree of congruence, thereby suggesting that the concrete's relative humidity response can be predicted by the established model. This provides a foundation for the optimal design of concrete with required mechanical properties in special applications.*

Key words: *Fractal dimension, Durability of concrete, Mathematical model, Moisture*

1. INTRODUCTION

Concrete is the most prevalent porous material utilized globally, and it is an enduring theme in mechanical engineering [1-3], and it might be also the very promising construction material in the Moon and the Mars by 3-D printing technology. The humidity within concrete plays a pivotal role in determining its mechanical, chemical, and thermal properties [4-6]. Consequently, the durability and reliability of concrete are significantly influenced by the transport of humidity within the concrete, especially for the recycled aggregate concretes. Given the vast quantity of demolished concrete waste present globally, the utilization of aggregates derived from this waste represents an environmentally friendly and cost-effective construction material.

Received: June 05, 2024 / Accepted July 20, 2024
Corresponding author: Hua-Wei Liu, Chao Liu
School of Civil Engineering, Xi'an University of Architecture and Technology, Xi'an, China
E-mails: liuhuawei@xauat.edu.cn (H. W. Liu); chaoliu@xauat.edu.cn (C. Liu)

In a surprising turn of events, the Telegraph reported in September 2023 that reinforced autoclaved aerated concrete (RAAC) had failed with only a lifespan of 30 to 40 years. This presents an urgent challenge for engineers and architects. This concrete material, which has been used in construction for decades, began to corrode and produce cracks. While this has caused some unfortunate accidents in the UK and other places, it has also led to some scientific discoveries. The primary factor contributing to its deterioration is the transformation of moisture, which results in corrosion. The volume of the corroded reinforcing steel bar can be increased by up to seven times [7], which is a remarkable phenomenon. The most concerning aspect is the absence of warning signs preceding damage, which further complicates the unpredictability of the failure.

Although there has been considerable research into the transport of moisture in concrete using differential models [8], there has been little investigation into the underlying mechanisms in fractal spaces. The fractal diffusion theory [9,10] represents an effective tool for the analysis of moisture transfer in concrete. The intricate micro/nano-structure of the pores can be represented by a fractal network [11-13]. In this paper, we will present a mathematical model in a two-scale fractal space, as described in Refs. [14-17].

2. FRACTAL MOISTURE TRANSFER

The intricate porosity structure within the concrete will result in a negative pressure, which will induce the evaporation of the absorbed water. This will initiate the process of moisture diffusion in concrete, as the concrete surface has the highest relative humidity, while the center has the lowest.

The diffusion process is a complex phenomenon that occurs in three dimensions [18]. In order to identify an analytical expression for this process, this paper examines the one-dimensional diffusion within concrete.

The porous concrete is treated as a two-scale fractal space, the fractal Fick's laws can be expressed, respectively, as

$$J = -D\frac{\partial^{\alpha} RH_D}{\partial^{\alpha} x} \tag{1}$$

$$\frac{\partial^{\alpha} RH_D}{\partial t^{\alpha}} = -\frac{\partial^{\alpha} J}{\partial x^{\alpha}} \tag{2}$$

where J is the diffusion flux, RH_D represents the relative humidity, D is the diffusion coefficient, α is the two-scale fractality for the porosity, and $\partial^{\alpha}/\partial t^{\alpha}$ is the two-scale fractal derivative.

So the fractal diffusion equation can be expressed as

$$\frac{\partial^{\alpha} RH_D}{\partial t^{\alpha}} = \frac{\partial^{\alpha}}{\partial x^{\alpha}}\left(D\frac{\partial^{\alpha} RH_D}{\partial x^{\alpha}}\right) \tag{3}$$

When α=1, Eq. (1) turns out to be the traditional Richards equation, which was used to study diffusion process in soils [19].

2.1. Initial Surface Absorption

When α=1, the initial surface absorption rates of water by the concrete can be expressed in the term of the Boltzmann variable [19]

$$I \propto t^{-1/2} \tag{4}$$

where I is the initial surface absorption rates, t is time. Nevertheless, Eq. (4) was found to be unsuitable for the concrete diffusion process. It should therefore be modified in accordance with the recommendation set out in [20]:

$$I \propto t^{-n} \tag{5}$$

where n is an experimental constant. In order to investigate the physical significance of the variable n in Eq. (5), it is possible to introduce a generalized Boltzmann variable in a manner analogous to that for the traditional Richards equation [19]:

$$\lambda = x^{\alpha} t^{-\alpha/2} \tag{6}$$

where λ is the generalized Boltzmann variable. The initial surface absorption rate on the concrete surface can be expressed as

$$I = at^{-\alpha/2} \tag{7}$$

where a is a constant.

The relationship between n and the fractality is therefore as follows

$$\alpha = 2n \tag{8}$$

Kumar and Bhattacharjee [20] denoted n as the silting factor, now we see that it is relative to two-scale fractal dimensions.

2.2. Fractal Diffusion in the Concrete

Following the initial surface absorption, the moisture diffuses from the concrete surface to the concrete interior. The diffusion process is primarily influenced by the geometry of the concrete pores.

In order to study the properties of Eq. (3) in more depth, the two-scale transform is introduced [21,22]

$$\begin{cases} s = t^{\alpha} \\ \xi = x^{\alpha} \end{cases} \tag{9}$$

Eq. (3) becomes

$$\frac{\partial RH_D}{\partial s} = \frac{\partial}{\partial \xi}(D\frac{\partial RH_D}{\partial \xi}) \tag{10}$$

The two-scale transform [21,22] is regarded as a physical interpretation of the fractional complex transform [23], which was originally proposed by Li & He [24]. It has been extensively employed in engineering, as evidenced by numerous references (see, for instance, Refs. [25-29]). The solution of Eq. (10) is

$$RH_D(\xi,s) = RH_\infty + (RH_0 - RH_\infty)\left[1 - \mathrm{erf}(\frac{1}{2}D^{-1/2}s^{-1/2}\xi)\right] \\ = RH_\infty + (RH_0 - RH_\infty)\,\mathrm{erfc}(\frac{1}{2}D^{-1/2}s^{-1/2}\xi) \tag{11}$$

where $RH_0=RH(0,t)$, $RH_\infty=RH(\infty,t)$, erf is the error function and erfc is the complementary error function. The solution of Eq. (1) is obtained as follows.

$$RH_D(x,t) = RH_\infty + (RH_0 - RH_\infty)\left[1 - \mathrm{erf}(\frac{1}{2}D^{-1/2}t^{-\alpha/2}x^\alpha)\right] \\ = RH_\infty + (RH_0 - RH_\infty)\,\mathrm{erfc}(\frac{1}{2}D^{-1/2}t^{-\alpha/2}x^\alpha) \tag{12}$$

The diffusion process is influenced by the pore structure of concrete, and the diffusion process in turn alters the pore structure of concrete. In order to investigate the relationship between the diffusion coefficient and the diffusion process with the pore properties of concrete, a dimensionless analysis [16,17,30] is employed in this paper.

The diffusion coefficient has a dimension of m^2/s. By means of dimensionless analysis, it can be assumed that

$$D = D(V_0, \frac{dRH_D}{dt}) \propto (V_0)^m (\frac{dRH_D}{dt})^n \tag{13}$$

Here V_0 is the pore volume, m and n are dimensionless exponents.

When $V_0 = 0$, there is no diffusion; and when $V_0 = 1$, diffusion can be studied using the traditional theory of thermodynamics. Furthermore, changes in relative humidity also affect the diffusion process, which ends when the diffusion process tends to be stabilized, that is to say when $dRH_D/dt=0$.

The dimensionless equation is

$$[L^2T^{-1}] = [L^{3m}T^{-n}] \tag{14}$$

That means

$$m = 2/3, n = 1 \tag{15}$$

We, therefore, obtain

$$D \propto (V_0)^{2/3}\frac{dRH_D}{dt} \tag{16}$$

The rate of change of relative humidity is related to saturation. When saturated ($\Theta=1$), $dRH_D/dt=0$. The rate of change of relative humidity is greatest when $\Theta=0$. Based on the above analysis, it can be assumed that

$$\frac{dRH_D}{dt} \propto (1-\Theta)^a \tag{17}$$

where a is the experimental constant. Also the pore volume is proportional to porosity:

$$V_0 \propto \varphi \tag{18}$$

Based on the above analyses, the following equations were obtained for the diffusion coefficient versus porosity and saturation degree

$$D = k\varphi^{2/3}(1-\Theta)^{a} \tag{19}$$

where φ is the concrete's porosity, k and a are experimental constants.

In literature, there was an empirical formula for soils' diffusion [31]:

$$D = c\varphi^{3/4}(1-\Theta)^{10/3} \tag{20}$$

Here c is a dimension-related parameter.

2.3. Fractal Permeation in the Concrete

In this paper, permeation is considered to occur when there is a pressure gradient, which is induced by the liquid-gas interface inside the concrete, the interface-induced force can be explained by the geometrical potential theory [32,33].

Darcy's law is the most basic tool for studying permeation phenomena, but it cannot analyze the effect of concrete pore properties (pore size and distribution) on permeation properties.

The fractal Darcy's law can be expressed as

$$Q = K\frac{A}{\mu}\frac{d^{\alpha}P}{dx^{\alpha}} \tag{21}$$

According to the definition of the fractal derivative, Eq. (21) can be approximated expressed as

$$Q = K\frac{A}{\mu}\frac{d^{\alpha}P}{dx^{\alpha}} = K\frac{A}{\mu}\lim_{\Delta x\to r}\frac{\Delta P}{(\Delta x)^{\alpha}} = K\frac{A}{\mu}\lim_{\Delta x\to r}\frac{\Delta P}{(\Delta x)^{\alpha}} \approx K\frac{A}{\mu}\Gamma(1+\alpha)r^{-\alpha+1}\frac{dP}{dx} \tag{22}$$

where Q is permeation flux, ΔP permeation pressure, r mean radius of pores, Γ gamma function, K permeability coefficient, A pore area, μ viscosity coefficient.

In the fractal space, the pore area scales as

$$A \propto r^{2\alpha} \tag{23}$$

The fractal Darcy's law can be expressed as

$$Q = -cr^{1+\alpha}\Delta P \tag{24}$$

where c is a constant.

The liquid-gas interface induced pressure can be described by the Kelvin equation [34]:

$$\Delta P = -\frac{\rho RT}{M}\ln RH_K \tag{25}$$

where RH_K is the relative humidity induced by the permeation process, R ideal gas constant (J/mol). M molar mass of water (kg/mol); T temperature (K); ρ density of water (kg/m).

Applying the approximate formula, ln(1+x)=x, the following approximate relationship can be obtained

$$\ln RH_K = \ln(1-(1-RH_K)) \approx -(1-RH_K) \tag{26}$$

Eq. (21) becomes

$$Q = cr^{1+\alpha}\frac{\rho RT}{M}\ln RH_K \approx -cr^{1+\alpha}\frac{\rho RT}{M}(1-RH_K) \tag{27}$$

According to the law of conservation of mass in the two-scale fractal space, we obtain that

$$\frac{\partial^\alpha(\rho\omega)}{\partial t^\alpha}+\frac{\partial^\alpha Q}{\partial x^\alpha}=0 \tag{28}$$

where ω is the ratio of water in liquid form to the total water in the concrete, it can be expressed as

$$\omega=\frac{V_{Water}}{V_{Water}+V_{Moisture}}=\frac{RH_K}{\Theta} \tag{29}$$

where V_{water} and $V_{Moisture}$ are, respectively the volume for water and moisture.

The mass conservation equation can then be written as

$$\frac{\partial^\alpha}{\partial t^\alpha}(\rho\frac{RH_K}{\Theta})-\frac{\partial^\alpha}{\partial x^\alpha}(cr^{1+\alpha}\frac{\rho RT}{M}(1-RH_K))=0 \tag{30}$$

or

$$\frac{\partial^\alpha}{\partial t^\alpha}(RH_K)+\frac{\partial^\alpha}{\partial x^\alpha}(D_c RH_K)=0 \tag{31}$$

Here D_c is given as follows

$$D_c = cr^{1+\alpha}\frac{RT\Theta}{M} \tag{32}$$

The general solution of Eq. (31) is

$$RH_K = f(x^\alpha - D_c t^\alpha) \tag{33}$$

where f is a continuous function. According to the initial and final conditions, we can get

$$\begin{aligned} RH_K(x,t) &= RH_\infty + (RH_0 - RH_\infty)\exp\left\{D_1(x^\alpha - D_c t^\alpha)\right\} \\ &= RH_\infty + (RH_0 - RH_\infty)\exp\left\{D_1(x^\alpha - cr^{1+\alpha}\frac{RT\Theta}{M}t^\alpha)\right\} \end{aligned} \tag{34}$$

where D_1 and c are experimental parameters.

2.4. Coupled Transport of Moisture Diffusion and Water Permeation

The processes of moisture diffusion and water permeation are studied separately in the aforementioned text, although they actually occur simultaneously. The relative humidity within the concrete can be approximately expressed as a result of the coupling of diffusion and permeation.

$$RH(x,t) = aRH_D(x,t) + (1-a)RH_K(x,t) \tag{35}$$

where *a* is the weight function, the early stage is dominated by diffusion, the final stage is dominated by permeation, assuming that at $t=t_0$, the diffusion and permeation contribute equally to *RH*, so we can choose the following weight function

$$a = \frac{t_0}{t+t_0} \tag{36}$$

where t_0 is determined according to the actual experiment. Thus we obtain the coupled transport equation

$$\begin{aligned} RH(x,t) &= \frac{t_0}{t+t_0} RH_D(x,t) + \frac{t}{t+t_0} RH_K(x,t) \\ &= \frac{t_0}{t+t_0}\left\{ RH_\infty + (RH_0 - RH_\infty)\left[1-\mathrm{erf}\left(\frac{1}{2}D^{-1/2}t^{-\alpha/2}x^\alpha\right)\right]\right\} \\ &+ \frac{t}{t+t_0}\left\{ RH_\infty + (RH_0 - RH_\infty)\exp\left[D_1\left(x^\alpha - cr^{1+\alpha}\frac{RT\Theta}{M}t^\alpha\right)\right]\right\} \end{aligned} \tag{37}$$

3. Theoretical Analysis

The experimental water box was designed with dimensions of 1000mm × 680mm × 600mm. The box was maintained at a temperature of 293 K (20 ℃), concrete samples were placed within the box for the purpose of measuring relative humidity at two locations, 2 cm and 4 cm beyond the concrete surface. The relative humidity was monitored at one-minute intervals until 2880 minutes had elapsed, the samples were tested for both the recycled aggregate concrete and natural aggregate concrete. Detailed experiment process was given in Ref. [35].

3.1. Humidity Response

According to the experiment data, we obtain the following humidity response:

$$\begin{cases} RH_{N-293-2} = 0.75840 + 0.24160\left[1-\mathrm{erf}(98.61t^{-0.4116})\right] \\ RH_{N-293-4} = 0.75739 + 0.24261\left[1-\mathrm{erf}(113.36t^{-0.4116})\right] \\ RH_{R-293-2} = 0.76545 + 0.23455\left[1-\mathrm{erf}(52.53t^{-0.35685})\right] \\ RH_{R-293-4} = 0.75289 + 0.24711\left[1-\mathrm{erf}(56.56t^{-0.35685})\right] \end{cases} \tag{38}$$

In the subscripts, *N* and *R* represent, respectively, natural aggregate concrete and recycled aggregate concrete. The value 293 represents temperature in Kelvin, while the values 2 and 4 represent, respectively, the depth from the concrete surface in centimeters.

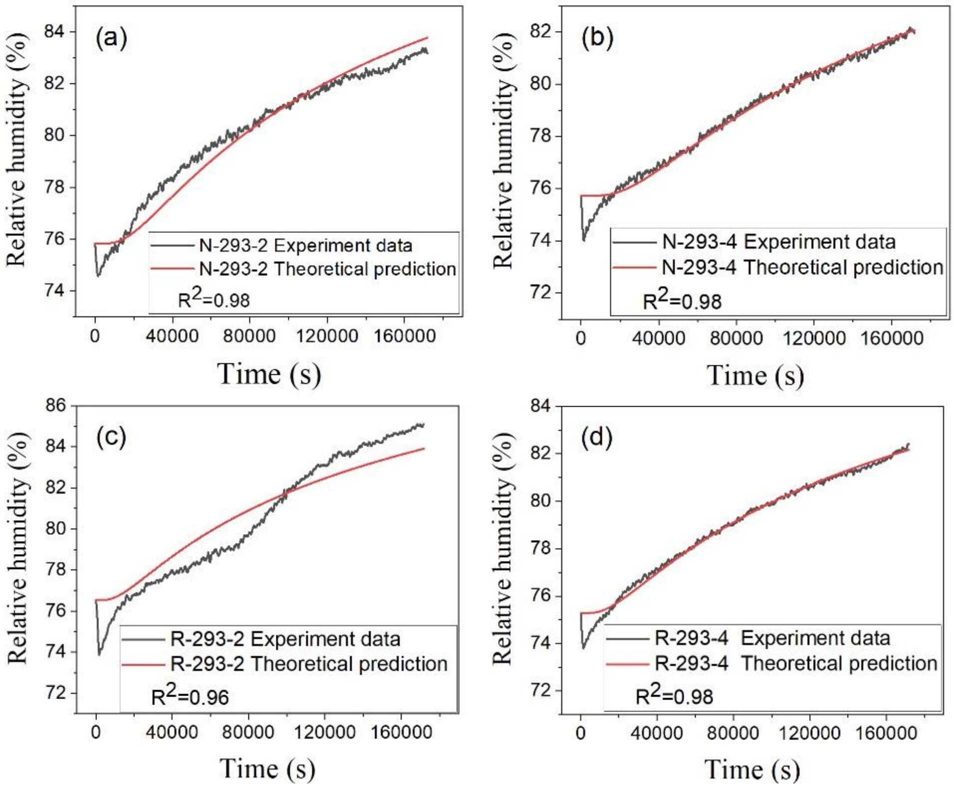

Fig. 1 Humidity change of concrete samples with temperature of 20 ℃ (293.15 K): Comparison between experimental results and calculated curves. (a)N-293-2; (b)N-293-4; (c)R-293-2; (d)R-293-4.

From Fig. 1, it can be seen that the experimental data basically match the theoretical results. The least squares fitting method was used in the curve fitting process, and because there is a sudden change in the initial response, the calculated curve does not have a good fit with the experimental curve, but the general trend is the same.

Sample R-293-2 appeared obviously two times response, the beginning of the response is slow, when t=10000s, the second response occurs. This is due to the diffusion-permeability coupling. Sample N-293-2 shows a similar situation, but it is not very obvious, with a faster response at the beginning, but the response becomes slower after t=100000 s. In contrast, samples N-293-4 and R-293-4 do not show the phenomenon of two responses, suggesting that diffusion dominates at x=4 cm, but it can be reasonably assumed that diffusion-permeability coupling will occur subsequently, the place near surface has a faster coupling than the center of the concrete.

3.2. Space Diffusion Process

According to the coefficients in Eq. (38), the average values of x=2 cm and x=4 cm are taken, and then re-fitting based on the experimental data gives the following results.

$$\begin{cases} RH_{N-293} = 0.75789 + 0.24211\left[1 - \mathrm{erf}(226.0301 t^{-0.4116} x^{0.2130})\right] \\ RH_{R-293} = 0.75917 + 0.24083\left[1 - \mathrm{erf}(132.0317 t^{-0.35685} x^{0.2472})\right] \end{cases} \quad (39)$$

According to the fitting results Eq. (39), Fig. 2 and Fig. 3 give the diffusion process of the specimens with time and space, and the trend is basically the same, but there are errors. The fitting results Eq. (39) indicate that water transport is not a simple one-dimensional transport problem, but is closer to three-dimensional transport.

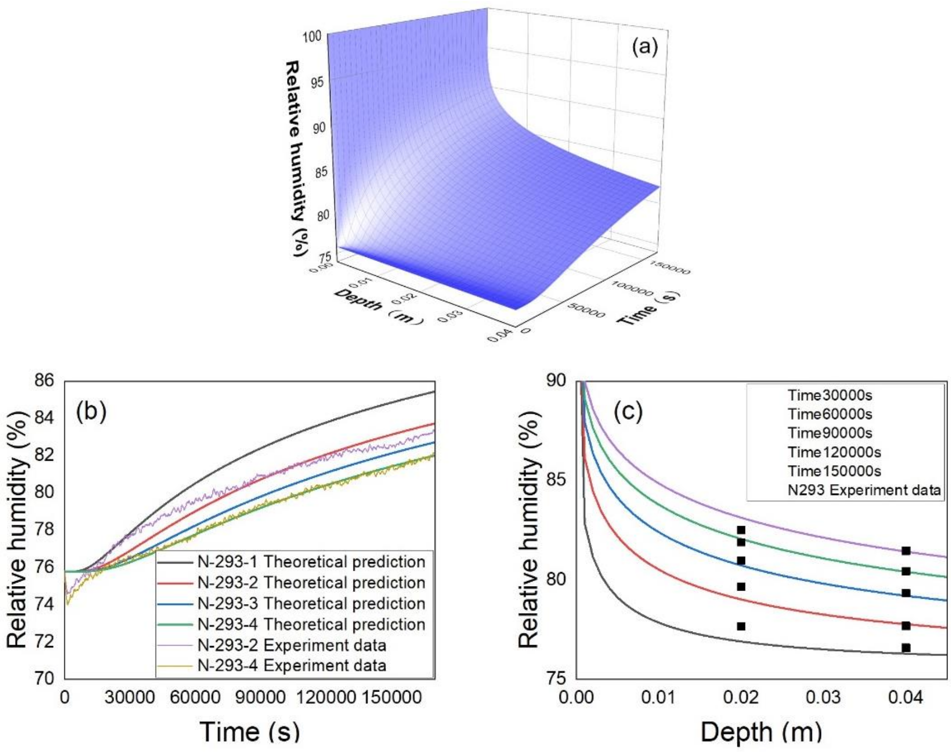

Fig. 2 Theoretical prediction for the diffusion process for the natural aggregate concrete at temperature of 20℃ (293.15K): (a) distance-time-relative humidity relationship; (b) time-relative humidity relationship; (c) distance-relative humidity relationship

Fig. 2 shows the diffusion process with time and depth for natural aggregate concrete at 20 °C (293.15 K). Since there are only two data sets for depth (x=2 cm and x=4 cm), there is a large deviation in the depth prediction. Fig. 2(b) shows that the fitted curves at x=2 cm and x=4 cm are in general agreement with the experimental data, and the trend for x=1 cm versus 3 cm is plotted according to Eq. (39). Fig. 2(c) shows that the relative humidity fits better at x=4 cm and shows a large error at x=2 cm for further improvement.

Fig. 3 shows the diffusion process with time and depth for the recycled aggregate concrete at 20 °C (293.15 K). Fig. 3(c) shows that the relative humidity is in good agreement at x=4 cm, with a large error at x=2 cm for further improvement.

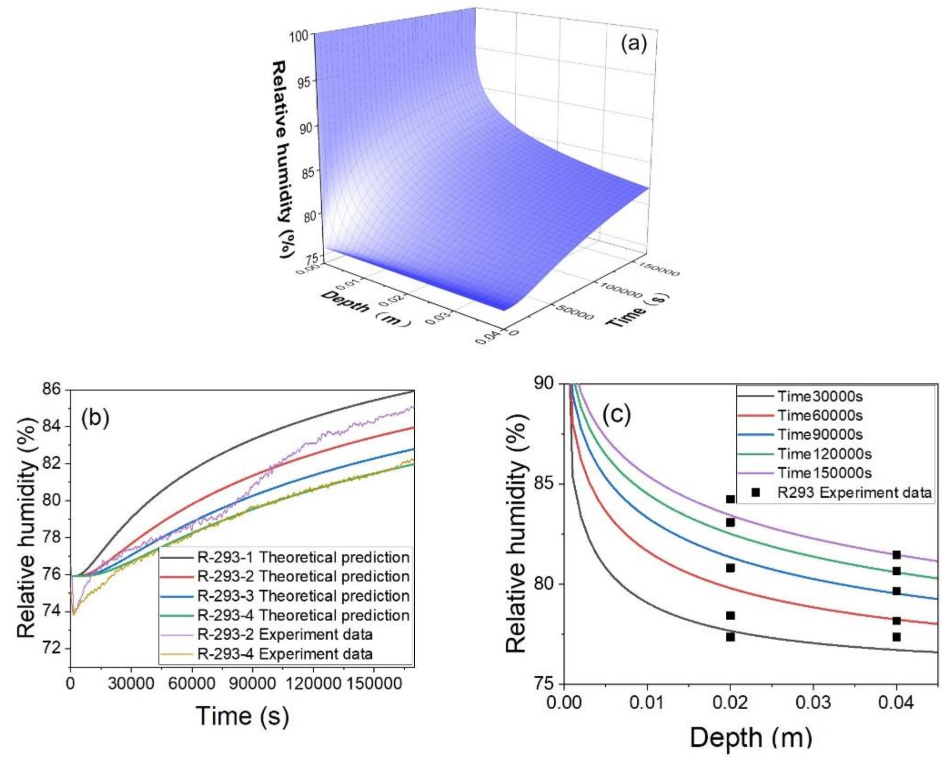

Fig. 3 Theoretical prediction for the diffusion process for the recycled aggregate concrete at temperature of 20 °C (293.15 K): (a) distance-time-relative humidity relationship; (b) time-relative humidity relationship; (c) distance-relative humidity relationship

3.3 Couple of the Fractal Diffusion Process and the Fractal Permeation Process

In view of the above analyses, the shallower the depth, the more likely to appear the coupling phenomenon of diffusion and permeation, in the depth of the farther, mainly diffusion is dominant. Considering both diffusion and permeation, the coupled transport equation for humidity is given as:

$$\begin{aligned} RH_{N-293}(x,t) &= \frac{10^5}{t+10^5}\left\{0.75789+0.24211\left[1-\mathrm{erf}(203.2086t^{-0.4116}x^{0.1914})\right]\right\} \\ &+\frac{t}{t+10^5}\left\{0.75789+0.24211\exp\left[-4.9741(x^{0.1914}-1.1797\times10^{-5}t^{0.8232})\right]\right\} \end{aligned} \tag{40}$$

$$RH_{R-293}(x,t)=\frac{10^5}{t+10^5}\left\{0.75917+0.2408\left[1-\mathrm{erf}(153.2464t^{-0.35685}x^{0.2237})\right]\right\}$$
$$+\frac{t}{t+10^5}\left\{0.75917+0.24083\exp\left[-5.0816(x^{0.2237}-5.2324\times10^{-5}t^{0.7137})\right]\right\} \quad (41)$$

In the case of water transport, diffusion is the dominant when $t < 10^5$. When $t > 10^5$, water transport is dominated by permeation. The calculation curves of the diffusion-permeability coupled transport model for each specimen are shown in Figs. 4 and 5.

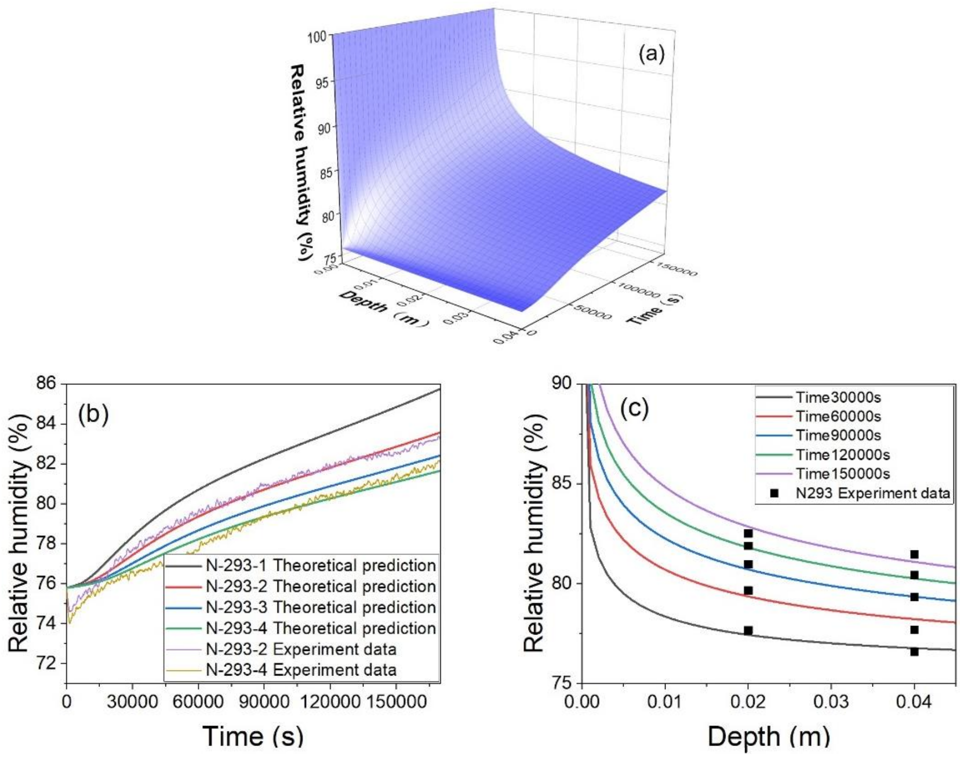

Fig. 4 Diffusion-permeability coupling for the natural aggregate concrete at temperature of 20 °C (293.15 K): (a) distance-time-relative humidity relationship; (b) time-relative humidity relationship; (c) distance-relative humidity relationship

Fig. 4 shows the calculated curves of the diffusion-permeability coupling model for natural aggregate concrete at 20 °C (293.15 K), and the overall fitting accuracies are relatively high to meet the engineering requirements. Fig. 4(b) shows that the fitted curves at x=2 cm and x=4 cm are in good agreement with the test data, so the predicted curves at x=1 cm and x=3 cm have some credibility. Fig. 4(c) also shows a significant improvement in accuracy at x=4 cm, indicating that the improved model has been used for engineering predictions, it can be a better illustration of the humidity response at t=3000 s, 6000 s, 9000 s, 12000 s and 15000 s, respectively.

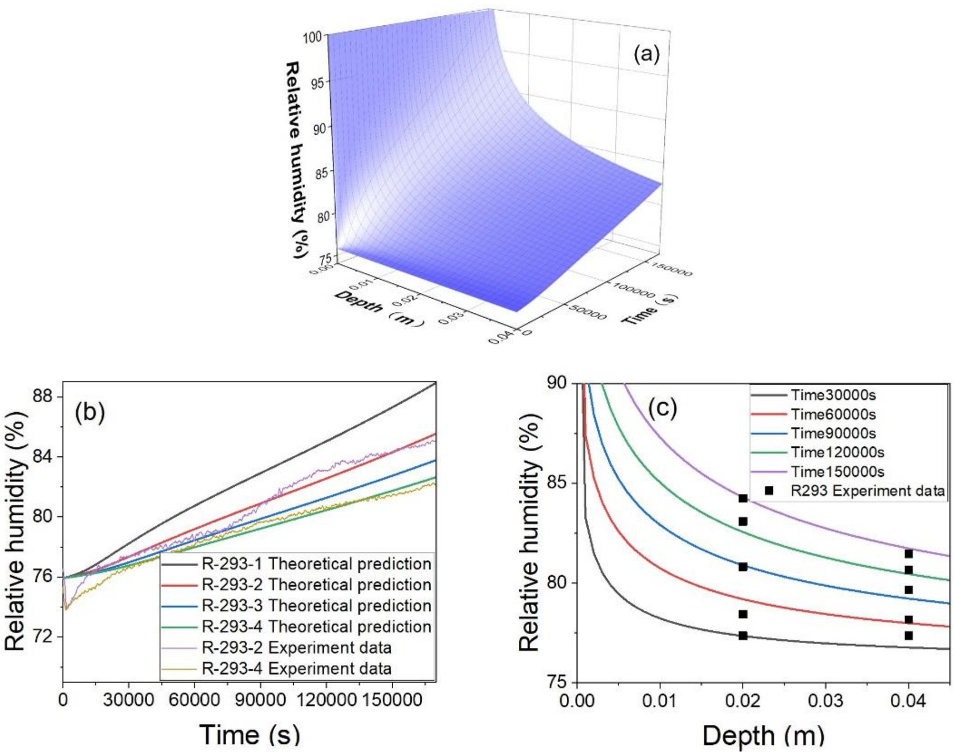

Fig. 5 Diffusion-permeability coupling for the recycled aggregate concrete at temperature of 20 ℃ (293.15 K): (a) distance-time-relative humidity relationship; (b) time-relative humidity relationship; (c) distance-relative humidity relationship

Fig. 5 shows the calculation curves of the diffusion-permeability coupling model of recycled aggregate concrete at 20 °C (293.15 K), and the overall fitting accuracy is also very good, and the accuracy basically meets the engineering requirements. Fig. 5(b) shows that the fitting curves at x=2 cm and x=4 cm have some deviation from the experimental data, which is mainly due to the special pore structure of recycled aggregate concrete and the internal interfaces, how to improve its accuracy needs further theoretical and experimental research. Fig. 5(c) also shows that the accuracy at x=2 cm needs to be further improved, which indicates that the closer to the surface of the concrete, the more obvious the penetration effect through the internal interface of recycled aggregate concrete.

In summary, the diffusion-permeability coupling model can fully show the relative humidity changing process with time and depth, and the fitted curve is basically consistent with the experimental data, which indicates that the moisture transport model established in this paper has a certain degree of credibility.

The diffusion-permeability coupling is a complex phenomenon. This paper employs weighting functions to decouple the two processes, thereby creating a framework for developing a comprehensive model of diffusion-permeability coupling in the future. Furthermore, the weighting functions may be enhanced by incorporating additional factors.

4. CONCLUSION

In this paper, the coupling mechanism of water vapor diffusion and permeation inside concrete is investigated based on the diffusion and permeation equations in the two-scale fractal space. The relative humidity response model of concrete was established, and its theoretical results were compared with experimental data, showing a high accuracy of the established model. The conclusions are as follows:

(1) This paper presents a new approach to fractal modifications of Fick's law and Darcy’s law in two-scale fractal space.

(2) A coupled model for the moisture diffusion and water permeation is proposed. Though the one-dimensional model is already doing a great job of predicting the internal humidity response characteristics of concrete, there is still plenty of room for improvement.

(3) The weight function is easy to determine based on the experimental data.

In order to leverage the potential of this approach, it is imperative that the mechanical field addresses the challenges of translating this theoretical analysis into practical applications.

The present theory offers a promising avenue for the design of porous concretes with the specified mechanical properties. Additionally, it offers a novel approach to addressing porous problems that arise in non-continuum mechanics, material science, and soil mechanics in the context of fractal space.

Acknowledgement: *The authors would like to acknowledge the National Natural Science Foundation of China (52178251 and 62276207), the Technology Innovation Guidance Program of Shaanxi Province (2023GXLH-049), the Qinchuangyuan’s "Scientist and Engineer" Team Building of Shaanxi Province (2023KXJ-242), the Special Research Program for Local Service of Shaanxi Province (23JC047), the Key Industry Chain Core Technology Tackling Project of Science and Technology Plan of Xi'an City (23ZDCYJSGG029-2022) for financial support.*

REFERENCES

1. Wang, J.H., Li, H.J., Ma, C. X., Cai, C.X., Wang, J.X., 2024, *Effect of surface curing condition on the humidity field and moisture transfer in concrete*, Construction and Building Materials, 411, 134701.
2. Gao, X.F., Yang, J., Shao, J.W., Zhu, H., Xu, J., Haruna, S.I., 2024, *Regulation of carbon nanotubes on internal humidity of concrete with recycled tire rubber: Mechanism analysis and modeling,* Journal of Building Engineering, 82, 108253.
3. Lyu, C., Xu, M., Lu, X.C., Tian, B., Chen, B.F., Xiong, B.B., Cheng, B., 2023, *Research on thermal-humidity-force coupling characteristics of mass concrete structures under temperature control,* Construction and Building Materials, 398, 132540.
4. Vishal, M., Satyanarayanan, K.S., 2024, *Effect of thermal expansion on three-dimensional reinforced concrete frames under high temperature,* Proceedings of the Institution of Mechanical Engineering Part C, 238(8), pp. 3240-3248.
5. Abdellahi, S.B., Hejazi, S.M., Hasani, H., 2022, *Investigation the influence of spacer yarns orientation angle on the thermal behavior of 3D textile reinforced concrete* (*TRC*), Proceedings of the Institution of Mechanical Engineers Part C, 236(8), pp. 4384-4393.
6. Praveen, V.J.M., Vigneshkumar, R., Karthikeyan, N., Gurumoorthi, A., Vijayakumar, R., Madhu, P., 2021, *Heat transfer enhancement of air-concrete thermal energy storage system-CFD simulation and experimental validation under transient condition,* Proceedings of the Institution of Mechanical Engineers Part E, 235(5), pp. 1304-1314.
7. O’Callaghan, J., 2023, *Why are concrete schools crumbling in the UK — and what can be done*?, Nature, 621, 242.

8. Hasan, A.M.R., Pillai, K.M., Zemajtis, F., Sobolev, K., 2023, *Modeling moisture infusion in ceramic using Richards equation: Experimental and analytical validations, and exploration of three time-dependent wetting scenarios*, Ceramics International, 49(23), pp. 39232-39248.
9. He, J.H., Qian, M.Y., 2022, *A fractal approach to the diffusion process of red ink in a saline water,* Thermal Science, 26(3B), pp. 2447-2451.
10. Qian, M.Y., He, J.H., 2022, *Two-scale thermal science for modern life –Making the impossible possible,* Thermal Science, 26(3B), pp. 2409-2412.
11. Babič, M., Marinkovic, D., Bonfanti, M., Calì, M., 2022, *Complexity modeling of steel-laser-hardened surface microstructures,* Applied Sciences, 12, 2458.
12. Babič, M., Marinković, D., 2023, *A new approach to determining the network fractality with application to robot-laser-hardened surfaces of materials,* Fractal and Fractional, 7(10), 710.
13. Babič, M., Marinković, D., Kovačič, M., Šter, B., Calì, M., 2022, *A new method of quantifying the complexity of fractal networks,* Fractal and Fractional, 6, 282.
14. He, C.H., Liu, C., He, J.H., Sedighi, H.M., Shokri, A., Gepreel, K.A., 2022, *A fractal model for the internal temperature response of a porous concrete,* Applied and Computational Mathematics, 21(1), pp. 71-77.
15. Anjum, N., Ain, Q.T., Li, X.X., 2021, *Two-scale mathematical model for tsunami wave,* GEM-International Journal on Geomathematics, 12(1), 10.
16. He, C.H., Liu, C., 2023, *Fractal dimensions of a porous concrete and its effect on the concrete's strength,* Facta Universitatis-Series Mechanical Engineering, 21(1), pp. 137-150.
17. He, C.H., Liu, S.H., Liu, C., Mohammad-Sedighi, H., 2022, *A novel bond stress-slip model for 3-D printed concretes,* Discrete and Continuous dynamical Systems-Series S, 15(7), pp. 1669-1683.
18. Li, X.X., Zhao, L., He, J.H., Zhou, C.J., Wu, S.G., Liu, Y., Wang, S.Q., 2023, *Temperature-dependent capillary rise and its effects on fabric cleaning and permeability,* Thermal Science, 27(3A), pp. 1915-1920.
19. Zhou, J., Liu, F.J. and He, J.H., 2013, *On Richards' equation for water transport in unsaturated soils and porous fabrics,* Computers and Geotechnics, 54, pp. 69-71.
20. Kumar, R., Bhattacharjee, B., 2004, *Assessment of permeation quality of concrete through mercury intrusion porosimetry,* Cement and Concrete Research, 34(2), pp. 321-328.
21. He, J.H., 2018, *Fractal calculus and its geometrical explanation,* Results in Physics, 10, pp. 272-276.
22. Zhao, L., Li, Y., He, J.H., 2023, *Promises and challenges of fractal thermodynamics,* Thermal Science, 27(3), pp. 1735-1740.
23. Ain, Q.T., He, J.H., Anjum, N., Ali, M., 2020, *The fractional complex transform: a novel approach to the time-fractional Schrodinger equation,* Fractals, 28(7), 2050141.
24. Li, Z.B., He, J.H., 2010, *Fractional complex transform for fractional differential equations,* Mathematical and Computation Applications, 15(5), pp. 970-973.
25. Zuo, Y. T., 2024, *Variational principle for a fractal lubrication problem*, Fractals, doi: 10.1142/S0218348X24500804.
26. Lu, J.F., Shen, S.W., Chen, L., 2024, *Variational approach for time-space fractal Bogoyavlenskii equation,* Alexandria Engineering Journal, 97, pp. 294-301.
27. Jiao, M.-L., He, J.-H., He, C.-H., Alsolami, A.A., 2024, *Variational principle for Schrödinger-KdV system with the M-fractional derivatives,* Journal of Computational Applied Mechanics, 55(2), pp. 235-241.
28. Elías-Zúñiga, A., Martínez-Romero, O., Trejo, D.O., Palacios-Pineda, L.M., 2022, *Analysis of a damped fractal system using the ancient Chinese algorithm and the two-scale fractal dimension transform*, Fractals, 30(9), 2250173.
29. Elías-Zúñiga, A., Martínez-Romero, O., Trejo, D.O., Palacios-pineda, L.M., 2024, *An efficient approach for solving the fractal, damped cubic-quintic Duffing's equation,* Fractals, 32(1), 2450011.
30. Estrada-Díaz, J. A., Olvera-Trejo, D., Elías-Zúñiga, A., Martínez-Romero, O., 2021, *A mathematical dimensionless model for electrohydrodynamics,* Results in Physics, 25, 104256.
31. Ray, N., Rupp, A., Schulz, R., Knabner, P., 2018, *Old and new approaches predicting the diffusion in porous media,* Transport in Porous Media, 124(3), pp. 803-824.
32. Fan, J., Zhang, Y., Liu, Y., Wang, Y.H., Cao, F.Y., Yang, Q.Q., Tian, F.M., 2019, *Explanation of the cell orientation in a nanofiber membrane by the geometric potential theory*, Results in Physics, 15, 102537.
33. Tian, D., Li, X.X., He, J.H., 2019, *Geometrical potential and nanofiber membrane's highly selective adsorption property,* Adsorption Science & Technology, 37(5-6), pp. 367-388.
34. Svintradze, D.V., 2020, *Generalization of the Kelvin equation for arbitrarily curved surfaces,* Physics Letters A, 84(20), 126412.
35. Liu, C., Liu, H.W., Zhu, C., Bai, G.L., 2019, *On the mechanism of internal temperature and humidity response of recycled aggregate concrete based on the recycled aggregate porous interface*, Cement and Concrete Composites, 103, pp. 22-35.